

**HEAT GENERATION AND TRANSPORT IN MICRO AND
SUB-MICRO SCALE IN ELECTRONIC PACKAGING**

by

OOI CHUN KEANG

Thesis submitted in fulfillment of the
requirements for the degree
of Master of Science

May 2003

ACKNOWLEDGEMENT

I would like to express my deepest gratitude to my supervisor Professor K.N. Seetharamu, for his tremendous guidance, advice, support, assistance and encouragement throughout my Master of Science programme. I also wish to express my sincere thanks to my co-supervisors, Dr. Zainal Alimuddin Zainal Alauddin for his help and support. I am also grateful to Intel Technology Sdn. Bhd. for providing the Intel Fellowship Grant and my Intel mentor Dr. Sim Kian Sin and Mr. Goh Teck Joo for their technical and moral support provided in completion of this project. Besides that, I would like to express my appreciation to Dr. Ghulam Abdul Quadir for his help and support. Last but not the least, my sincere thanks, compliment and regards to whom for help and support me in my efforts.

C.K. Ooi

February 2003

LIST OF CONTENTS

ACKNOWLEDGEMENT	ii
LIST OF CONTENTS	iii
LIST OF FIGURES	viii
LIST OF TABLES	xiii
NOMENCLATURE	xiv
ABSTRAK	xvii
ABSTRACT	xviii
CHAPTER 1: INTRODUCTION	1
1.1 Introduction of electronic packaging	1
1.2 Thermal management in electronic packaging	5
1.3 Present thermal management problems	6
1.4 Project objective	6
1.5 Thesis outline	7
CHAPTER 2: LITERATURE SURVEY	8
2.1 Overview	8
2.2 Non-Fourier heat conduction analysis	8
2.2.1 Short-time heating analysis	9
2.2.2 Numerical modeling of microscale heat conduction	15

LIST OF CONTENTS

ACKNOWLEDGEMENT	ii
LIST OF CONTENTS	iii
LIST OF FIGURES	viii
LIST OF TABLES	xiii
NOMENCLATURE	xiv
ABSTRAK	xvii
ABSTRACT	xviii
CHAPTER 1: INTRODUCTION	1
1.1 Introduction of electronic packaging	1
1.2 Thermal management in electronic packaging	5
1.3 Present thermal management problems	6
1.4 Project objective	6
1.5 Thesis outline	7
CHAPTER 2: LITERATURE SURVEY	8
2.1 Overview	8
2.2 Non-Fourier heat conduction analysis	8
2.2.1 Short-time heating analysis	9
2.2.2 Numerical modeling of microscale heat conduction	15

2.3 High speed Very-Large-Scale-Integrated (VLSI) interconnection	17
2.4 Asymptotic Waveform Evaluation (AWE) scheme	18
CHAPTER 3: NON-FOURIER HEAT CONDUCTION MODEL	22
3.1 Overview	22
3.2 Introduction	22
3.3 Development of three-dimensional heat conduction equation	23
3.4 Finite element formulation	25
3.5 Implementation of boundary conditions	35
3.5.1 Specific temperature boundary conditions	35
a) Gradual rise of temperature	35
b) Instantaneously rise of temperature	36
3.5.2 Constant heat flux boundary conditions	36
3.5.3 Convection boundary conditions	37
3.6 Fourth order Runge-Kutta method	37
3.7 Verification of methodology	39
CHAPTER 4: VERY-LARGE-SCALE-INTEGRATED (VLSI) INTERCONNECTION THERMAL ANALYSIS	42
4.1 Overview	42
4.2 Introduction of ESD/EOS	42
4.3 Modeling of high speed VLSI interconnection	43
4.4 Verification of methodology	51

CHAPTER 5: FAST TRANSIENT THERMAL ANALYSIS	53
5.1 Overview	53
5.2 Introduction of fast transient analysis scheme	53
5.3 Concepts of Asymptotic Waveform Evaluation (AWE)	54
5.4 Definition of moments	55
5.5 Solution for ordinary differential equation (ODE)	55
a) First order ordinary differential equation (1 st ODE)	55
b) Second order ordinary differential equation (2 nd ODE)	57
5.6 Transient response for system	62
5.7 Verification of methodology	63
a) RC network system	63
b) Circular fin system	66
CHAPTER 6: RESULTS AND DISCUSSION	69
6.1 Overview	69
6.2 Analysis of three-dimensional Non-Fourier heat conduction model	69
6.2.1 Specific temperature boundary conditions	69
6.2.2 Effect of thermal behavior	71
6.2.3 Effect of Temperature gradient phase lag τ_T	74
6.2.4 Effect of initial temperature rate	75
6.3 Analysis of high speed VLSI interconnection	78
6.3.1 Effect of duty cycle	78
6.3.2 Comparison of hyperbolic and parabolic model	80
6.3.3 Effect of metal line width	81
6.3.4 Effect of current density	82

6.4 AWE transient thermal analysis	85
6.4.1 Application of AWE in fin analysis	86
a) Nodes stability analysis	86
b) Comparison with 4 th order Runge-Kutta method	87
c) Comparison of CPU time	88
d) Effect of moment approximation	91
6.4.2 Application of AWE in micro-channel heat exchanger system	92
a) Effect of heat transfer coefficient for different flow constraints	94
b) Effect of heat loading	95
c) Temperature distribution for fluid	97
6.4.3 Application of AWE in mechanical vibration system	97
6.4.4 Application of AWE in hyperbolic model analysis	101
CHAPTER 7: CONCLUSION	105
7.1 Overview	105
7.2 Non-Fourier heat conduction model	106
7.3 Very-large-scale-integrated (VLSI) interconnection thermal analysis	106
7.4 Fast transient thermal analysis	107
7.5 Recommendations for future works	107
REFERENCES	108
APPENDICES	115
APPENDIX A: Response of a system to various inputs	116
APPENDIX B: Modify Nodal Analysis (MNA) formulation for RC network	117

LIST OF CONTENTS

APPENDIX C: Formulation for Circular Fin thermal analysis	118
APPENDIX D: Formulation for micro-channel heat exchanger system	119
APPENDIX E: Gauss elimination method	122
PUBLICATION LIST	124

LIST OF FIGURES

	Page
Figure 1.1 Hierarchy in electronic packaging	3
Figure 1.2 (a) Electronic packaging configuration for Ball-Grid Arrays (BGA)	4
Figure 1.2 (b) Electronic packaging configurations for Multichip Modules (MCM)	4
Figure 1.2 (c) Electronic packaging configurations for Flip-Chips	4
Figure 1.2 (d) Electronic packaging configurations for Chip-on-Board	5
Figure 1.2 (e) Electronic packaging configurations for Chip Scale Packages (CSP)	5
Figure 3.1 Three-dimensional simple rectangular bar model with meshing	25
Figure 3.2 Node numbering in tetrahedral element	26
Figure 3.3 Element division of one-half of the cube	29
Figure 3.4 The delay in gradual rise temperature boundary conditions	36
Figure 3.5 Gradual rise of temperature at center line for time 0.05 ($z_q=0.05$, total nodes=1000)	40
Figure 3.6 Instantaneous rise of temperature at center line for time 0.05 ($z_q=0.05$, total nodes=1000)	41

Figure 4.1	(a) Interconnect of length l between two identical inverters (b) Equivalent distributed RC representation	43
Figure 4.2	Location of metal interconnection in IC chip	44
Figure 4.3	(a) MOS cell diagram for the IC chip (b) Interconnect metal in IC chip	44
Figure 4.4	(a) Cross-section of real VLSI interconnect structure (b) A schematic cross-section of a multilevel VLSI interconnect	45
Figure 4.5	A unipolar pulsed waveform during ESD conditions	49
Figure 4.6	Heat generation in single level TiN/Al(Cu)/TiN structure	50
Figure 4.7	Comparison of experimental data and present model with various current pulses (ambient temperature of 25°C).	52
Figure 5.1	Concept of Model Order Reduction technique to speed up the simulation	54
Figure 5.2	7 nodes of RC network system	64
Figure 5.3	Comparison for present and Chiprout et. al. (1994) for input pulse waveform of 0.1 ns rise/fall time and 0.3 ns duration	65
Figure 5.4	Comparison for present scheme and Matlab-Simulink™ for input pulse waveform of 0.3 ns and 0.5ns duration	65
Figure 5.5	Geometry representation of real structure fin model	66
Figure 5.6	Comparison of AWE approximation with 4 th Order Runge Kutta method, numerical integration method and ANSYS [®]	67
Figure 6.1	Comparison of the model for thermal diffusion case in instantaneous rise temperature boundary condition	70

Figure 6.2	Comparison of the model for thermal diffusion case in gradual rise temperature boundary condition	71
Figure 6.3	Temperature distribution for gradual rise boundary condition	73
Figure 6.4	Temperature distribution for instantaneous rise boundary condition	73
Figure 6.5	Effects of temperature gradient phase lag (τ_T) to temperature distribution	75
Figure 6.6	Temperature distribution for initial temperature rate $\dot{\theta} = 0$	76
Figure 6.7	Temperature distribution for initial temperature rate $\dot{\theta} = 5$	76
Figure 6.8	Temperature distribution for initial temperature rate $\dot{\theta} = 25$	77
Figure 6.9	Temperature distribution for initial temperature rate $\dot{\theta} = 50$	77
Figure 6.10	Effect of duty factor to peak temperature	78
Figure 6.11	Transient response of level one interconnect at duty cycle of 40%	79
Figure 6.12	Transient temperature responses compared for hyperbolic model and parabolic model	80
Figure 6.13	Effect of metal line width for duty factor of 100% and 50%	82
Figure 6.14	Comparison of present methodology with experimental data for current pulse of 200ns	83
Figure 6.15	Interconnects temperature distributions for various current densities at current pulse of 100ns	84
Figure 6.16	Interconnects temperature distributions for various current densities at current pulse of 200ns	84

LIST OF FIGURES

Figure 6.17	Interconnects temperature distributions for various current densities at current pulse of 300ns	85
Figure 6.18	Transient temperature response with different nodes	86
Figure 6.19	Comparison of 2 nd order AWE approximation with 4 th Order Runge-Kutta at three different locations in the fin system	88
Figure 6.20	Comparison of CPU time for AWE scheme and 4 th Order Runge-Kutta	89
Figure 6.21	Significant short computational time with current scheme even for large size problem	90
Figure 6.22	The effect of total number of nodes to the temperature distribution	90
Figure 6.23	The effect of moment approximation to temperature profiles	92
Figure 6.24	Microchannel heat sink with boundary conditions apply	92
Figure 6.25	Details and FEM representation of microchannel heat sink	93
Figure 6.26	Transient responses of the maximum dimensionless temperature for different values of heat transfer coefficient	94
Figure 6.27	Transient responses for different values of heat loading	96
Figure 6.28	Temperature distribution along fluid flow	97
Figure 6.29	Two degree of freedom system	98
Figure 6.30	Transient vibration response for mass number one	99
Figure 6.31	Transient vibration response for mass number two	99
Figure 6.32	Transient vibration response with damping applied for mass number one	100

LIST OF FIGURES

Figure 6.33	Transient vibration response with damping applied for mass number two	100
Figure 6.34	Schematic of problem geometry and boundary conditions	102
Figure 6.35	Temperature comparison for one, three moments AWE approximation and Runge-Kutta method	103
Figure 6.36	Temperature distribution as a function of time for rectangular bar model	104

LIST OF TABLES

		Page
Table 3.1	Nodes and numbering connectivity in tetrahedral element	26
Table 3.2	Element division for six tetrahedral elements	29
Table 4.1	Dimension for Al(Cu) interconnection	46
Table 4.2	Material property for Al(Cu) interconnection	47
Table 4.3	Data for temperature dependent term and defect term for Al(Cu) interconnection	48
Table 5.1	Results comparisons with ANSYS [®] , 4 th Order Runge-Kutta Method and Logan at time $t=3s$	68
Table 6.1	Steady state results comparison for Gauss elimination, Runge-Kutta and AWE scheme	87
Table 6.2	Simulation parameters for microchannel heat sink	93
Table 6.3	CPU time and steady state temperature comparison for different values of heat transfer coefficient	95
Table 6.4	CPU time and steady state temperature comparison for different values of heat loading	96
Table 6.5	Vibration amplitude and time step comparison for Runge-Kutta method and AWE scheme	101
Table 6.6	Results comparison for hyperbolic analysis at time $t=5$	103

NOMENCLATURE

Symbol	Description	Unit
Bi	Biot number	-
c	Specific heat	J/kg.K
C	Thermal wave speed	m/s
C_ϕ	Capacitance	pF
e_ϕ	Excitation vector	-
f	Carrier distribution function	-
f_0	Equilibrium distribution	-
F_λ	External driving force	N
h	Height of model	m
h_c	Heat transfer coefficient	W/m ² . K
I_{RMS}	Current root-means-square	A
k	Thermal conductivity	W/m. K
l	Length of model	m
M_{xy-z}	Expression for estimation time step	s
O_p	Order of approximation	-
P	Power	W
q	Non-dimensional heat flux	-
Q	Heat flux	W/m ²
Q_g	Volumetric heat generation rate	W/m ³

NOMENCLATURE

r	Space variable	m
R	Resistivity	$\mu\Omega\cdot\text{cm}$
t	Time	s
T	Temperature	K
T_{∞}	Ambient temperature	K
T_w	Wall temperature	K
v_x	Carrier group velocity	m/s
V	Volume for tetrahedron element	m^3
w	Width of model	m
x,y,z	Spatial coordinate	m
z_q	Non-dimensional phase lag for heat flux	-
z_T	Non-dimensional phase lag for temperature gradient	-

Greek Notations

α	Thermal diffusivity	m^2/s
β	Non-dimensional time	-
β_r	Non-dimensional time for gradual rise temperature boundary condition	-
Δt	Time step	s
θ	Non-dimensional temperature	-
μ	Non-dimensional absorption coefficient	-
δ	Non-dimensional x distance	-
ξ	Non-dimensional y distance	-
γ	Non-dimensional z distance	-

NOMENCLATURE

ρ	Density	Kg/m^3
$\rho_{\text{line}}(T,c)$	Resistivity of metal interconnect	$\mu\Omega\cdot\text{cm}$
$\rho_{\text{pure}}(T)$	Temperature dependent resistivity	$\mu\Omega\cdot\text{cm}$
$\rho_{\text{def}}(c)$	Defect resistivity	$\mu\Omega\cdot\text{cm}$
τ_q	Phase lag for heat flux	s
τ_T	Phase lag for temperature gradient	s
τ_{e}	Mean relaxation time	s
χ	Diffusivity	m^2/s

**PENJANAAN DAN PEMINDAHAN HABA DALAM SKALA MIKRO DAN
SUB-MIKRO UNTUK PEMBUNGKUSAN ELEKTRONIK**

ABSTRAK

Semasa proses pembungkusan micro elektrik, penukaran tenaga berlaku dalam dimensi dan masa yang kecil. Oleh itu, semasa proses pemanasan pantas, hukum Fourier adalah tidak memadai untuk menerangkan fenomena ini. Maka hukum alternatif yang dinamakan sebagai hukum Non-Fourier telah diperkenalkan. Hukum Non-Fourier berdasarkan kepada model ekoran dua fasa telah memperkenalkan dua anggapan yang baru untuk mengatasi dua kelemahan dari hukum Fourier semasa pemanasan pantas. Anggapan ini ialah halaju peresapan terma adalah terhad dan wujud masa pengimbangan antara elektron dan kekisi. Hanya satu persamaan menakluk dalam model ekoran dua fasa telah memadai untuk menerangkan semua keadaan sempadan. Ekoran fasa ini ialah fasa untuk kecerunan suhu (τ_T) dan fluks haba (τ_q). Kaedah unsur terhingga dan Rungke-Kutta digunakan untuk membangun model Non-Fourier dalam tiga-dimensi dan suhu yang diperolehi adalah kurang berbanding dengan satu dan dua dimensi. Penggunaan model ekoran dua fasa dalam analisis very large scale integrated (VLSI), menunjukkan kegagalan litar berlaku pada denyutan arus 300ns. Aplikasi kaedah Asymptotic Waveform Evaluation (AWE) dalam tertib pertama dan kedua persamaan perbezaan biasa menunjukkan satu pencapaian yang menakjubkan jika dibandingkan dengan kaedah penyelesaian yang biasa. Kaedah yang canggih, pantas dan berkesan ini menunjukkan kepututsan yang baik berbanding dengan kaedah Runge-Kutta, kaedah time integration, kaedah central difference dan ANSYS⁹⁶, tetapi ia lebih pantas.

ABSTRACT

Energy exchange takes place in extremely small dimension and time scale in the process of micro-electronic packaging. For fast heating response, Fourier conduction law is inadequate to explain the phenomena. Thus, an alternative law is introduced to compensate the Fourier law, named as Non-Fourier law. Non-Fourier law, based on two-phase-lag model has introduced two new assumptions, to eliminate the drawbacks from classical Fourier heat conduction equation when applied to rapid heating process. These assumptions are finite thermal wave propagation speeds and time of equilibrium between electron and lattice. From previous research on dual phase-lag model, different governing equations have to employ for different boundary conditions, but with a proposed two phase-lag model only a single governing equation is adequate. These phase lags are the phase lag for temperature gradient (τ_T) and heat flux (τ_q). A finite element method and Runge-Kutta method are applied in the development of three-dimensional Non-Fourier heat conduction model. Three-dimensional model predicted a lower temperature values as compared with one-dimensional and two-dimensional model. The application of two phase-lag model to very-large-scale-integrated (VLSI) interconnect thermal analysis, illustrates that circuit open failure occurs at current pulse of 300ns. An implementation of Asymptotic Waveform Evaluation (AWE) scheme in first and second order ordinary differential equation shows a break through as compared with conventional methods. This advanced, powerful and efficient scheme shows excellent results compared with Runge-Kutta method, central difference method and ANSYS[®] 5.4, and is several orders faster.

CHAPTER I

INTRODUCTION

1.1 Introduction to electronic packaging

Recently, the trend in reducing the size of electronic devices to sub-micrometer range make the electrical and thermal phenomena become significant. Energy exchange over extremely small dimension and time scales are significant in the process of micro-electronic packaging. This microelectronics typically refers to those micro devices, such as integrated circuits, which are fabricated in sub-micron dimensions and which form the basis of all electronic products. The growth of markets for sophisticated electronic products into submicron-scale and the increase in integrated circuit capability have created a situation whereby the electronic packaging technology must rapidly improve in order to maintain the overall momentum of the vast electronics-based industries. Packaging focuses primarily on how chips may be packaged cost-effectively and reliably. Electronic packaging is the technology of packaging electronic devices and it refers to:

- The packaging of the integrated circuit chips.
- The interconnections (both on and off the chips) for signal and power transmission.
- The encapsulations for protecting the chips and interconnections from moisture, chlorides, and other species in the environment
- The heat sinks or other cooling devices needed to remove heat from the chips.
- The power supply

- The housing for electromagnetic interference (EMI) shielding.

An electronic packaging configuration typically consists of component packages containing silicon die (chips), and other components such as capacitors and resistors, mounted on printed circuit boards. These printed circuit boards with components (call modules) are then mounted in a chassis that provides protection from the environment, cooling, mechanical support, and a method of interfacing to the outside world. Because of differences in materials and configurations requiring a different approach, an electronic packaging configuration is frequently broken down into a series of hierarchy. Electronic packaging has its conventional hierarchy as show in the figure 1.1 (Tummala, 2001).

Level 1: Either single or multi-chip modules

Level 2: Printed circuit board (PCB)

Level 3: Packaging for motherboard

By undergoing the packaging process as described above an electronic package eventually will assemble into a final product. The major functions of the electronic package are as shown below:

- To provide a path for the electrical current that powers the circuits on the IC chip.
- To distribute the signal onto and off the IC chip.
- To remove the heat generated by the circuits on the IC chip
- To support and protect the IC chip from hostile environments.

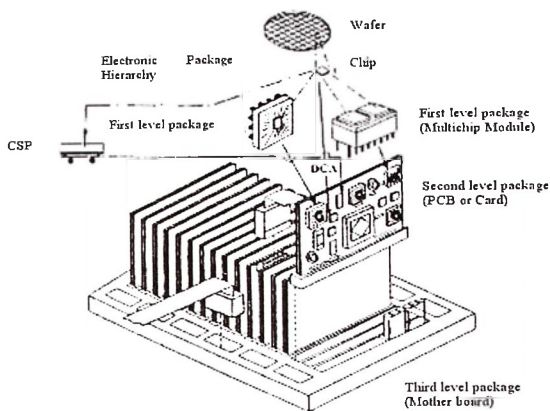


Figure 1.1: Hierarchy in electronic packaging

Although the above packaging levels are frequently used, they are not universal. Increasing packaging density and the use of novel packaging approaches (such as multichip modules and chip on board) have often clouded the distinction between the packaging levels. The increase in reliability and efficiency of electronic packaging technology has enhanced the development of some electronic packaging configurations in the past few years that may require special consideration. Specifically, these configurations include Ball-Grid Arrays (BGA), Multichip Modules (MCM), Chip Scale packages (CSP), Flip-Chips and Chip-on-Board. Use of the above configurations may require special considerations in thermal, stress, delamination, vibration and solder life analyses. The details of the above packaging configurations are shown in the figure 1.2.

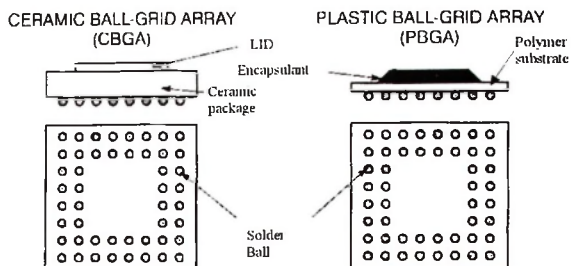


Figure 1.2 (a): Electronic packaging configurations for Ball-Grid Arrays (BGA)

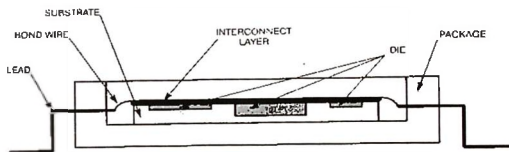


Figure 1.2 (b): Electronic packaging configurations for Multichip Modules (MCM)

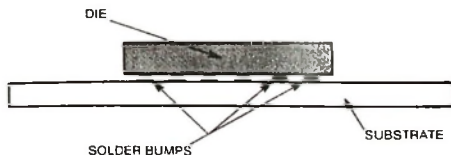


Figure 1.2 (c): Electronic packaging configurations for Flip-Chips

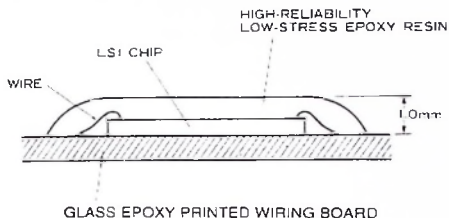


Figure 1.2 (d): Electronic packaging configurations for Chip-on-Board

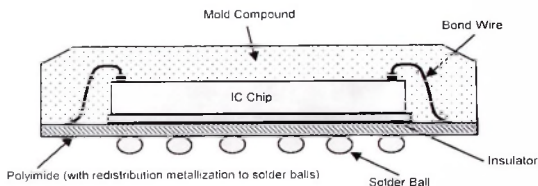


Figure 1.2 (e): Electronic packaging configurations for Chip Scale Packages (CSP)

1.2 Thermal management in electronic packaging

The goal of thermal management is typically to determine junction temperature of the electronic components for reliability assessment and to ensure that manufacture's rating is met. An additional goal is to evaluate top-level thermal management for use in determining environmental and cooling requirements. Electronic packaging configurations are typically increasing in performance and speed while decreasing in size, resulting in greatly increased power density. As a result, thermal management is essential to determine the thermal path and the applicable heat transfer mechanisms.

1.3 Present thermal management problems

Thermal management is becoming increasingly challenging, due to the rapid increase of heat dissipation from logic modules, and the trend of shrinking systems physical size. From the research of thermal design engineer in past, temperature distribution is determined as most challenging issues in thermal management, because it determines the service life of electronic components. Excessively high temperature degrades the chemical and structural integrity of various materials used in the equipment. Large fluctuations of temperature as well as large spatial variations of temperature in the equipment become responsible for malfunction and eventual breakdown of the equipment. In industries more than 50% of the failure in the electronic packages are temperature dependent, thus a good thermal management in electronic packaging systems is essential.

1.4 Project Objectives

There are three objectives in this analysis of heat generation and transport in micro and sub-micro scale in electronic packaging, which are listed below:

- To develop a three-dimensional model with Non-Fourier conduction equation to predict temperature for short response.
- To simulate the self-heating effect in Very-Large-Scale-Integration (VLSI) interconnections.
- To introduce a fast solution scheme for transient thermal analysis, named as Asymptotic Waveform Evaluation (AWE) scheme, which gives solutions at desired locations only (local solution).

1.5 Thesis outline

The thesis is presented in seven chapters including introduction, literature survey, analysis of Non-Fourier heat conduction model, analysis of high speed Very-Large-Scale Integration (VLSI) interconnection thermal study, fast transient thermal analysis and finally results and discussion and conclusion. The first chapter will give a clear objective of the project, an overview of the concept of electronic packaging and the introduction of new model to improve the current classical heat conduction model. In chapter two a literature review regarding Non-Fourier model, VLSI interconnection simulation and AWE scheme, is presented. In this chapter the definition and the concept of several terms are discussed in details. The fundamental theory of finite element method, methodology and numerical approach used to simulate the Non-Fourier model are presented in chapter three. In chapter four, the transient simulation results of VLSI interconnection with current Non-Fourier model are described. A powerful, faster and advanced transient solution scheme is introduced in chapter five with its details to implement this new scheme. The results from chapter three, four and five are presented and discussed in chapter six. Finally the thesis ends up with conclusions in chapter seven.

CHAPTER 2

LITERATURE SURVEY

2.1 Overview

Literatures reviews for three main scopes of the thesis are presented in this section.

These scopes are shows as below:

- Non-Fourier heat conduction analysis
- High speed Very-Large-Scale-Integrated (VLSI) interconnection
- Asymptotic Waveform Evaluation (AWE) scheme

2.2 Non-Fourier heat conduction analysis

As the size of semiconductor devices reduce, effectiveness heat removal from a devices become a critical issue for packaging technology. For microscale heat transfer the individual heat carriers eg., phonons, electrons and photons, may dramatically affect the observed temperature behavior. In metals, both free electrons and phonons transfer heat energy while in semiconductors the phonons are the major heat carriers. The individual heat carriers travel an average distance, or mean free path in a material before transmitting their energy to other heat carriers by collisions. Collision between electrons and lattice will lead to heat generation in semiconductor devices. During collision, the lattice temperature increases because lattice gains energy from electron during collision. The energy exchange processes in micro-electronic devices take extremely small dimensions and time scales, thus for fast heating response non-Fourier conduction effects have to take into account for the accurate estimation of heat transfer rates. Classical Fourier law based on the diffusion model (parabolic conduction model) with

assumption of thermal propagation speeds is infinite and simultaneous development of heat flux and temperature gradient for most analysis is appropriate. But, for rapid heating process Fourier law becomes inadequate to describe the phenomena. Various models have been proposed to eliminate two drawbacks from classical Fourier heat conduction equation when applied to rapid heating process.

2.2.1 Short-time heating analysis

Boltzmann's equation which governs the distribution function for both molecules in gas, and free electrons and phonons which are modeled as heat carriers in solids is important in the historical development of heat waves and is credited first to Ward and Wilks (1951, 1952), for deriving the second sound speed and the temperature wave equation for liquid Helium II. Boltzmann's equation is given as.

$$\frac{\partial f}{\partial t} + v_x \frac{\partial f}{\partial x} = -\frac{f - f_0}{\tau_{cs}} \quad (2.1)$$

Morse and Feshbach (1953), Cattaneo (1958) and Vernotte (1961) have introduced their models to eliminate the Fourier law drawbacks. Morse and Feshbach (1953) have first incorporated the finite propagation speed which lead to a hyperbolic heat conduction equation. Cattaneo (1958) and Vernotte (1961) proposed a macroscopic thermal wave model, which leads to a hyperbolic heat conduction equation and suggesting a finite speed propagation of heat. The expression for temperature from Cattaneo (1958) and Vernotte (1961) is given as.

$$\tau \frac{\partial^2 T}{\partial t^2} + \frac{\partial T}{\partial t} = \chi \frac{\partial^2 T}{\partial x^2} \quad (2.2)$$

Tavernier (1962) introduced a mean relaxation time, τ in deriving a heat flux equation of the Cattaneo type for solids. The modified heat flux equation from Boltzman's transport equation was presented as.

$$q = -k \frac{\partial T}{\partial x} - \tau \frac{\partial q}{\partial t} \quad (2.3)$$

Boltzman's transport equations is given as.

$$\frac{\partial f}{\partial t} + v_x \frac{\partial f}{\partial x} + \frac{F_x}{m} \frac{\partial f}{\partial v_x} = \left[\frac{\partial f}{\partial t} \right]_{scattering} \quad (2.4)$$

By approximating the scattering term as $\left[\frac{\partial f}{\partial t} \right]_{scattering} = -\frac{f - f_0}{\tau_v}$, the hyperbolic heat conduction equation was obtained. The Boltzman's equation is also the starting point in the work of Guyer and Krumhansl (1964) who employed the Callaway difference approximation using two time of relaxation for the scattering term than the one-term approximation employed in Tavernier (1962). Maurer (1969) derived a hyperbolic heat conduction model for metals. Its predictions are significantly different from those predicted from the parabolic Fourier model.

From a microscopic viewpoint, Anisimov et. al. (1974), was the first who developed a microscopic two-step model in predicting the rapid transient responses. This model considers the laser radiation heating process in two steps, that is, the absorption of photon energy by electrons and heating of the lattice through electron-phonon coupling. This model is an example where the phonon-electron interaction dominates the short-time heat transfer before diffusion. By appropriate mathematical manipulations, the microscopic two-step model may be combined for the determination of lattice or electrons temperatures respectively. This effort has been further advanced subsequently in Fujimoto et. al. (1984), Brorson et. al. (1987) and Elsayed-Ali (1991). A hyperbolic

heat conduction model have been carried out in the analysis of thermal wave propagation subjected to various time dependent flux boundary conditions, by Vick and Ozisik (1983), Glass et. al. (1985), Orlande and Ozisik (1994), Chen (1999) and Fushinobu et. al. (1995).

Qiu and Tien (1992) proposed a two-step model to capture the temperature profile during rapid heating process. The proposed model predicted a much lower lattice temperature rise and a larger heat affected area as compared with conventional one-step heating model. These differences could be very important in processes in which the temperature and the size of heated area need to be precisely controlled. The two-step model also reveals that the microscopic photon-electron and electron-phonon interactions are major contribution in delaying the lattice response to the heating pulse.

Qiu and Tien (1993) have made a comment on Fourier law regarding the assumption of simultaneous development of heat flux and temperature gradient. This assumption will lead to the instantaneous local thermal equilibrium occurring between electrons and the atomic lattice. But, Qiu and Tien (1993) found that if large energy fluxes are deposited onto a metallic substrate in the form of electromagnetic radiation, the temperature for electron rise faster than lattice because of faster photons-electron interaction. Moreover, a finite relaxation time is required for local thermal equilibrium to be established between the electrons and phonons (atoms of the lattice). Thus, Qiu and Tien (1993) have solved the Boltzmann equations and proposed a hyperbolic two-step radiation-heating model, where phonon-electron dominates the heat transport in rapid heating analysis. From the analysis of Qiu and Tien (1993) it shows the proposed two-step model agrees well with experimental data but the parabolic two-step model fails to

predict a finite speed of energy propagation. Tzou (1993) suggested the use of single phase-lag concept in rapid heating analysis. This new concept reveals the non-equilibrium thermodynamic transition problem from macroscopic point of view.

$$Q(\mathbf{r}, t + \tau_q) = -k \nabla T(\mathbf{r}, t) \quad (2.5)$$

equation above account for the phase lag between the heat flux and the temperature gradient τ_q . As the phase lag is very small, equation (2.3) reduces to exponential relaxation model with the phase lag being the relaxation time. But, the concept proposed by Tzou (1993) didn't account for the finite thermal relaxation time for the electrons and lattice to reach local thermal equilibrium.

Tzou (1995) proposed a universal constitutive equation between the heat flux and the temperature gradient to cover the behavior of diffusion (macroscopic in both space and time), wave (macroscopic in space but microscopic in time), and pure phonon scattering for one-dimensional model analysis. The model is generalized from the dual-phase-lag concept accounting for the lagging behavior in the high-rate response. While the phase lag of the heat flux captures the small-scale response in time, the phase lag of the temperature gradient captures the small-scale response in space. The effects of non-equilibrium thermodynamic transition and the microscopic effect in the energy exchange are accounted in the model. The microstructural effects had lumped into the delay response in time in the macroscopic formulation. A generalized form of heat flux equation was established, which could predict all the heat conduction behaviors in the microscopic models. Thus, dual-phase-lag concept makes the transition from a macroscopic analysis to a microscopic evaluation much smoother and more efficient. The constitutive equation proposed by Tzou (1995) to describe the lagging behavior is.

$$q(\mathbf{r}, t + \tau_q) = -k \nabla T(\mathbf{r}, t + \tau_T) \quad (2.6)$$

From the analysis of Tzou (1995) it is shown that the classical Fourier (diffusion) theory deviates most from his model because classical Fourier law does not incorporate any small-scale effect like, phonon-electron interactions. Tzou (1995) also indicated that the small-scale response in space and time couldn't be separated. Although, the wave theory aims to capture the small-scale response in time (in terms of τ_q), it does not seem to be complete until the microscale response in space (in terms of τ_T) is implemented.

Instead of the classic Fourier equation based on diffusion, Guo and Xu (1995) used a hyperbolic equation based on a wave model to predict the rapid transient heat conduction in IC chips. Guo and Xu (1995) applied the non-Fourier heat conduction equation derived by Cattaneo (1958) and Vernotte (1961) and compared with the classical Fourier heat conduction equation in rapid heating analysis. A hyperbolic equation predicted a higher peak temperature and thermal stress, greater temperature difference between components as compared with classical Fourier heat conduction equation. Tang and Araki (1996) compared their macroscopic heat flux relaxation model which lead to hyperbolic equation (thermal wave model) with microscopic two-step model, which was first developed by Anisimov et. al. (1974). This comparison shows that the temperature response predicted by hyperbolic model is located at the place between the two (electron and lattice temperatures) predicted by two-step model.

A three-dimensional laser-heating model by taking into account the phase change process was proposed by Yilbas and Sami (1998). Electron-kinetic theory was employed in the analysis of laser heating and governing equations are solved numerically. It is observed that the three-dimensional model proposed predicted a lower surface temperature as compared with that predicted from one-dimensional model.

Kathy and Haji-Sheikh (1999) and Tang and Araki (1999) have applied Green's function method in high-speed heating analysis. Kathy and Haji-Sheikh (1999) modified the Green's function and this equation employs a lagging behavior similar to Tzou (1995) and agrees with the hyperbolic two-step model for metals. From the analysis it shows that the hyperbolic model predicted a higher phase angle while the two-step model predicted a lower phase angle than the Fourier conduction model. Tang and Araki (1999) have derived an analytical solution of the generalized heat conduction equation for one-dimensional model by using Green's function method and finite integral transform technique. This analytical solution is in the same form of generalized heat flux equation that has been derived by Tzou (1995). For metals, by comparing with the microscopic two-step model derived by Anisimov et. al. (1974), Tang and Araki (1999) found that τ_q captures the relaxation behavior of electron-thermal wave conduction, while τ_T captures the effect of phonon-electron interaction.

Al-Nimr et. al. (2000) applied dual-phase-lag heat conduction model in non-equilibrium entropy production. It is shown that the entropy production cannot be described using the classical form of the equilibrium entropy production where using this form leads to a violation of the thermodynamics second law. The dual-phase-lag allows either the temperature gradient (cause) to precede the heat flux vector (effect) or the heat flux vector (cause) to precede the temperature gradient (effect) in the transient process. Wang and Prasad (2000) and Hadj-Taieb and Lili (2000) have further studied the capability of hyperbolic model. Wang and Prasad (2000) take into account the effects of microscale, non-Fourier diffusion heat and mass transfer and non-equilibrium kinetics in the analysis of non-equilibrium phase change in rapid solidification. Whereas, Hadj-Taieb and Lili (2000) implemented hyperbolic model in the analysis of transient flow of

homogeneous gas-liquid mixtures. By applying the conservation of mass and momentum laws, a nonlinear hyperbolic system of two differential equations is obtained for the two principal dependent variables, which are the fluid pressure and velocity.

2.2.2 Numerical modeling of microscale heat conduction

Both Prakash et. al. (2000) and Zhang and Zhao (2001a) applied the two phase-lag model in one-dimensional microscale heat conduction analysis, but Zhang and Zhao (2001a) only provided a solution scheme named as fourth order compact finite difference scheme used with a Crank-Nicholson type integrator. The new scheme is compared with existing scheme based on second order spatial discretization. It is shown that the new scheme is computationally more efficient and more accurate than the second order scheme. But Prakash et. al. (2000), applied boundary conditions other than prescribed surface temperature, and such studies have not been considered in the literature before. Prakash et. al. (2000), found out the available closed-form solutions for the dual-phase-lag model to be widely different for apparently similar boundary conditions. From the study, the origin of the discrepancy in the available analytical results from Lin et. al. (1997) and Tzou (1995) has been identified as the sensitivity of the predicted solution to the way of implementing the surface boundary conditions. The differences occur because Lin et. al. (1997) applied instantaneously constant temperature rise boundary condition in his analytical solution, while Tzou (1995) imposed rapid continuous rise of temperature boundary condition in his analytical solution. The wave and diffusion solution for heat flux boundary conditions agree well with the corresponding analytical solutions of the simple hyperbolic conduction equation proposed by Wiggert (1977). The phenomena of thermal wave, pure diffusion and over diffusion subjected to various boundary conditions have been carried out in the

analysis of Prakash et. al. (2000). Besides that, Prakash et. al. (2000) also employed two phase-lag model in laser pulse heating of a thin metallic plate together with the effect of pulsation frequency on dynamics of temperature variation. A numerical solution with finite element method and fourth order Runge-Kutta time marching method has been employed by Prakash et. al. (2000) for the spatial and temporal discretisations in the analysis.

Cheah et. al. (2000) and Zhang and Zhao (2001b) have extended the one-dimensional two-phase-lag model analysis into two-dimensional microscale heat conduction analysis. Zhang and Zhao (2001b) only proposed an efficient numerical strategy to solve the governing equation, a second order finite difference scheme in both time and space is introduced and the unconditional stability of the finite difference scheme is proved. A computational procedure is designed to solve the discretized linear system at each time step by using a preconditioned Conjugate Gradient method. The computational procedure proposed has been verified by the numerical experiments to be efficient and accurate. One step ahead the two-dimensional model, Zhang and Zhao (2001c) proposed the same solution scheme for three-dimensional model. Cheah et. al. (2000), have extended the effort of Prakash et. al. (2000) to study the effect of two-dimensional microscale heat conduction analysis. The two-dimensional analysis is performed with various boundary conditions such as instantaneous and gradual rise of temperature, convection, constant heat flux and pulse laser heating. From the analysis it is shown that temperature profiles predicted from two-dimensional two phase-lag model are lower than that predicted from one-dimensional model obtained by Prakash et. al. (2000).

2.3 High speed Very-Large-Scale-Integrated (VLSI) interconnection

Short-time high joule heating cause thermal break down of metal interconnects in electrostatic discharge (ESD) and electrical overstress (EOS) protection circuits and I/O buffers have shown a reliability concern. Shingubara et. al. (1995) have performed a molecular dynamics simulation of the behavior of a void in Al interconnect with a bamboo grain boundary under a high DC current stress. It is shown that when the current density is higher than some threshold value, a void can move across the grain boundary transversely without being trapped in it, and a disordered region is formed between a void and grain boundary after the transverse process. Banerjee et. al. (1997), developed a model incorporating the heating layered metal system with the oxide surrounding it. The model is shown to be in excellent agreement with experimental results and is applied to generate design guidelines for ESD/EOS and I/O buffer interconnects.

Rzepka et. al. (1998) employed FEM software ANSYS[®] in the analysis of very-large-scale-integrated (VLSI) interconnection. It is shown during EDS/EOS, a single, very short but huge pulse strikes interconnects thus electromigration lifetime is therefore not the primary concern but melting that could open those lines. The effect of self-heating of interconnect has been shown to affect the lifetime of integrated circuits significantly, an open circuit failure occurs even for current pulses of 300ns width. Voldman (1998), Murarka (1997) and Brillouet (1997), have proposed and possible materials solutions to meet the future challenges.

Banerjee and Hu (1998) modeled the non-linear I-V characteristics of silicide films under DC and pulsed high current stress and the non-linearity has been shown to be due

to self-heating. Srikar and Thompson (2000) and Bohm et. al. (2002), have performed the failure analysis due to electromigration in Al interconnection. Interaction of stress-relief induced crystallographic defects with translating erosion voids to cause a transition to slit-like void shapes been shown to be energetically feasible.

Banerjee et. al. (2000) and Gonzalez et. al. (2000) presented a detailed microanalysis of interconnect failure mechanisms under short-pulse stress conditions arising during peak current and ESD events. Banerjee et. al. (2000) employed a three-dimensional thermo-mechanical model to account for the open circuit failure mode at which the passivation layers are fractured. The direct evidence of latent damage in AlCu lines stressed under high current short-pulse conditions has been presented for the first time. Streiter et. al. (2002) studied the thermal and electrical behaviour of interconnects for the 100nm and 50nm technology node, and it is shown that the maximum possible current density of DC line is determined by a self-consistent approach considering both joule heating and electromigration.

2.4 Asymptotic Waveform Evaluation (AWE) scheme

The inspiration of this concept first came from the research of Rubinstein et. al. (1983). They are doing the research in the RC-trees network simulation by using the efficient Elmore delay (first moment of the impulse response) estimate approach. But this estimate approach has not always produced an accurate result, because there are a lot of limitations in doing a transient analysis. So, the major effort of the early work was to find a solution scheme for transient analysis.

The work from McCormick (1989), gave a second spark to this concept. From his research in interconnect circuit simulation, he has shown that the circuit moments (the coefficient of expansion of circuit driving point of transfer function in a Maclaurin series about $s=0$ in the frequency domain) could lead to lower circuit models and reasonably accurate transient response results. From the previous effort of these authors in formalization and generalization of the algorithm, eventually an n^{th} order extension of the first order Elmore delay approximation was developed and named as AWE. With this new scheme, the response of the higher order systems can be simulated by the low order of approximation. These approximations consist of a few dominant poles (and zeros) in the Pade approximation, so as the order of approximation increase, the corresponding approximate transient response will asymptotically approach to the actual response, thus the nature of the approximation itself eventually inspiring the name.

From the literature this scheme was used to be a generalized approach for approximating the dominant poles and zeros for linear circuits, with the poles and zeros generated from this scheme the transient response of circuit can be obtained. AWE also provided a delay evaluation methodology for RLC circuit interconnect models, linear active and passive circuits in electrical field. Pillage et. al. (1990) attempted to apply this scheme in circuits with floating nodes (capacitor cut sets) analysis, the responses predicted from first order approximation of AWE show a good agreement with the actual response.

Same year, Pillage and Rohrer (1990) again show a capability of this scheme in transient analysis. In the analysis, this scheme is applied to capture the effect of interconnect on the delay with a simplified model, typically a RC tree model and this

scheme produced reasonable results as compared with SPICE™ simulation but, two or three orders faster than SPICE™. From their work, it shows this scheme is applicable in floating node, linear controlled sources, finite input rise time, charge sharing, bipolar circuitry, interconnect timing estimation and MOS circuit analysis. Lee et. al. (1992) coupled this scheme with adjoint sensitivity method to study the circuit parameters and parasitics, and excellent matches to the exact response from HSPICE™ simulation are obtained. Smith and Das (1995) used a lumped-pi or lumped-tee systems in the EMC analysis of electrical interconnects, again a good agreement with conventional SPICE™ simulation is obtained.

Gong and Volakis (1996) show this scheme is an extremely useful for computing wideband frequency response with only a few samples of the system solution. Tutuianu et. al. (1996) in RC-circuit delay analysis, shows only 1% of differences exist between AWE scheme and analytical solutions but AWE is more powerful in high-speed interconnect circuit simulation. Zhu et. al. (2001) with present scheme reveal that peak crosstalk voltage is over 60% larger for 5 GHz high-speed interconnects than predicted by current distributed RC models. Slone et. al. (2001) proposed to couple Galerkin method and AWE to solve FEM equations in electromagnetic radiation analysis. The proposed method shows a good agreement with LU decomposition method.

From literature review, it is noticed that almost all the works are either analytical on one-dimensional analysis, or only a few are engaged in numerical finite element method and two-dimensional microscale heat conduction analysis. Thus, from the motivation of Prakash et. al. (2000) and Cheah et. al. (2000), an effort is put to extend the micro-scale heat conduction with two phase-lag model in three-dimensional model analysis. The

present two phase-lag model will also cover the transient thermal analysis of short-time heating for VLSI interconnection during electrostatic discharge (ESD) conditions.

All previous research using AWE only involved first order ordinary differential equation (1st ODE) and initial conditions are not incorporated. However, to make this scheme applicable in thermal analysis, the effect of initial conditions is essential. Da et. al. (1995) presented a first paper in Printed-circuit board (PCB) thermal analysis using AWE scheme, but the response formulation, poles and residues used to predict the transient temperature response for first order ordinary differential equation (1st ODE) seem to be incorrect and no details described to incorporate the initial conditions. Thus, in this research project, AWE scheme is extended to incorporate the effect of initial conditions and to provide a solution for first order ordinary differential equation (1st ODE) and second order ordinary differential equation (2nd ODE) in transient thermal analysis.

CHAPTER 3

NON-FOURIER HEAT CONDUCTION MODEL

3.1 Overview

In this section various approaches used to achieve the objectives will be dealt. The topics included in this chapter are shown as below.

- Development of three-dimensional finite element model
- Finite element formulation
- Implementation of boundary conditions
- Fourth order Runge-Kutta scheme
- Verification of methodology

3.2 Introduction

A powerful simulation tool Matlab R12 (Biran and Breiner, 1995) is used in this project to perform all the simulation tasks. This simulation tool is selected because of its simplification and efficiency in the programming part as compared to other conventional programming software such as Visual Basic 6.0 and C/C++ programming. In addition, Matlab R12 is a powerful tool to handle matrices algebra, thus it enhanced the analysis of FEM in solving huge matrices after the meshing process. Furthermore, Graphical user interface (GUI) tools and built in powerful analysis tools, make Matlab extremely powerful tool for solving problems in many fields. Thus, this program is selected to develop the programming codes for three-dimensional non-Fourier heat conduction model.

3.3 Development of three-dimensional heat conduction equation

Non-Fourier heat conduction equation with the two-phase lag, and finite element method (FEM) for spatial variation are implemented in the project to establish the three-dimensional model study. In order to get the solution for the transient analysis a numerical method, fourth order Runge-Kutta time marching method is used. The results from three-dimensional model will be compared with one-dimensional results from Prakash et. al. (2000) and two-dimensional model from Cheah et. al. (2000) to show the need of three-dimensional model. From the research work of Prakash et. al. (2000) and Cheah et. al. (2000), even though the results predicted from them are in good agreement with literature, but most engineering problems are three dimensional. Thus in order to obtain more reasonable and realistic result; a three-dimensional model has been implemented. The equation for three-dimensional with two phase-lag model is (Tzou 1995).

$$Q(x, y, z, t + \tau_q) = -k \nabla T(x, y, z, t + \tau_T) \quad (3.1)$$

The constitutive relation between the heat flux and temperature gradient of the two-phase lag model in equation (3.1), can be expanded using Taylor series. The expansion is given in the equation below:

$$\begin{aligned} Q(x, y, z, t) + \tau_q \frac{\partial Q}{\partial t}(x, y, z, t) + \frac{(\tau_q)^2}{2!} \frac{\partial^2 Q}{\partial t^2}(x, y, z, t) + \dots \\ = -k \left[\nabla T(x, y, z, t) + \tau_T \frac{\partial \nabla T}{\partial t}(x, y, z, t) + \frac{(\tau_T)^2}{2!} \frac{\partial^2 \nabla T}{\partial t^2}(x, y, z, t) + \dots \right] \end{aligned} \quad (3.2)$$

This expansion is performed by assuming the phase lag for temperature gradient τ_T and phase lag for heat flux τ_q are very small and higher order terms in the expansion are negligible. The assumption above eventually lead to the simplified form as follows:

$$Q(x, y, z, t) + \tau_q \frac{\partial Q}{\partial t}(x, y, z, t) = -k \left[\nabla T(x, y, z, t) + \tau_T \frac{\partial \nabla T}{\partial t}(x, y, z, t) \right] \quad (3.3)$$

By using the equation (3.3) above and performing an energy balance over an infinitesimal control volume, the following form of the generalised heat conduction equation can be obtained (Tzou 1995).

$$\frac{\partial^2 T}{\partial x^2} + \frac{\partial^2 T}{\partial y^2} + \frac{\partial^2 T}{\partial z^2} + \tau_1 \left[\frac{\partial^3 T}{\partial t \partial x^2} + \frac{\partial^3 T}{\partial t \partial y^2} + \frac{\partial^3 T}{\partial t \partial z^2} \right] = \frac{1}{\alpha} \frac{\partial T}{\partial t} + \tau_q \frac{1}{\alpha} \frac{\partial^2 T}{\partial t^2} \quad (3.4)$$

The relation for τ_q with thermal wave speed (C) is given in the expression below

$$\frac{\tau_q}{\alpha} = \frac{1}{C} \quad (3.5)$$

The thermal diffusivity is given as

$$\alpha = \frac{k}{\rho c} \quad (3.6)$$

In order to perform an analysis in three-dimensional case, a simple rectangular bar of height h , length l and width w is selected for the present analysis as shown in figure 3.1. Figure 3.1 shows a sketch of the rectangular bar, the five surfaces of the bar are subjected to various boundary conditions such as prescribed temperature, constant heat flux and convective heat transfer. At the right end of the bar, the spatial gradient of temperature is assumed to be zero, because that surface is insulated. From the literature of Tzou (1995) and Lin et. al. (1997) it has been shown that the solution of the problems is affected by the prescribed values of both T and \dot{T} at the starting boundary. A non-dimensionalisation is performed for the equation (3.4) above, in order to compare with the non-dimensional results produced by Prakash et. al. (2000) and Cheah et. al. (2000). Using the following variables the procedure of non-dimensionalisation is carried out.

$$\theta = \frac{T - T_0}{T_w - T}, \beta = \frac{t}{l^2/\alpha}, \delta = \frac{x}{l}, \xi = \frac{y}{h}, \gamma = \frac{z}{w}, z_T = \frac{\tau_1}{l^2/\alpha} \text{ and } z_q = \frac{\tau_q}{l^2/\alpha} \quad (3.7)$$